Australian Journal of Basic and Applied Sciences, 3(4): 4644-4655, 2009
ISSN 1991-8178

Programmed Cell Death in the Liver of Different Species of Anuran Amphibians During Metamorphosis

Abdel Hakim Saad, Ahmed Abdel Aziz, Ibrahim Yehia, Abdel Wahab El-Ghareeb, and Hamida Ismail

Department of Zoology, Faculty of Science, Cairo University.

Abstract: In all processes of vertebrate postembryonic development, amphibian metamorphosis displays the most prominent transformation, which includes the typical programmed cell death in regressing or remodeling organs. Programmed cell death or apoptosis plays a key role in liver development and homeostasis. In the present study, induction of liver apoptosis in the four tested species of anuran amphibians (*Bufo regularis, Bufo viridis, Rana bedriagae* and *Ptychadena mascareniesis*) during metamorphosis showed both the morphological and the biochemical features typical of mature apoptotic cells. Hematoxylin and eosin staining revealed that the apoptotic hepatic cells shrunk, leaving a gap with cell borders, and they featured pyknotic nuclei and condensed chromatin, recognizable as apoptotic bodies. Ultrastructural examination using the electron microscopy, the chromatin was condensed and aggregated in sharply delineated, uniformly dense masses, which in some cases were seen on the inner surface of the nuclear membrane. The nuclear membrane was clearly intact, as were the cellular membranes. Budding of the nucleus to produce discrete nuclear fragments of varying size and chromatin content, which surrounded by double membranes, was also detected. Organelles remain well preserved and the mitochondria were clearly identifiable at this time. These features are typical of apoptotic cells and were observed in the four anuran species during prometamorphosis till the end of climax. In order to confirm the morphological signs of apoptosis, pulsed-field gel electrophoresis indicated the formation of high molecular weight fragments ranging from 1.5 Mb to 73 Kb in length. Strong and weak smears of high molecular weight DNA could be observed in all samples. Our results identify similar events because liver is included in anuran tissue preparations that were used for histological analysis, and because liver apoptosis that occurs during metamorphosis appears to involve some evolutionarily conserved biological processes.

Key words: Apoptosis, Anura, Metamorphosis, Liver,light,microscopy, Electron microscopy, DNA fragments

INTRODUCTION

Apoptosis plays an important role in the normal development and homeostasis of metazoans (Arends and Wyllie, 1991; Hale *et al*., 1996; Kornbluth and Evans, 2001; Tsuchiya *et al*., 2005; Kloc *et al*., 2007). To study the molecular mechanisms involved in the regulation of this basic phenomenon, cell-free systems produced from *Xenopus laevis* have recently been widely used (Knapp *et al*., 2006; Fujimoto *et al*., 2007; Taniguchi *et al*., 2008). Although this cell-free system provides useful biochemical model to study the activation of apoptosis, studies on the histological, biochemical and molecular basis regulating programmed cell death (PCD) in amphibians have been very limited. For this reason, we decided to study PCD in a physiological context, such as ontogenic development or metamorphosis of frogs and toads. Cell death is known to occur in this setting, but its nature and mechanisms are completely unknown (Furlow and Neff, 2006; Knapp *et al*., 2006; Skirrow and Helbing, 2007).

Bufonidae and *Ranidae* represent the two largest anuran families with over 700 species distributed in all parts of the world except for Antarctica (Amphibia Web, 2004). *Bufo* and *Rana* comprise the largest genus with over 300 species. In Egypt, these diverse groups are exemplified by *Bufo regularis*, *Bufo viridis*, *Rana bedriagae* and *Ptychadena Mascareniesis*. The geographic distribution of *Bufo* and *Rana* displays an extensive native and introduced range that includes; North America, as well as locations in South America, Europe and Asia (GloblInvasive-Species-Database). Due to their habitation, *Bufonidae* and *Ranidae* are frequently used as important families in experimental biology studies.In the present study, we demonstratedthat induction of liver apoptosis in the four tested species of Egyptian anuran amphibians during metamorphosis showed both the morphological and the biochemical features typical of mature apoptotic cells.

Corresponding Author: Ahmed Abdel Aziz, Department of Zoology, Faculty of Science, Cairo University.
E-mail: abdelaziz.baiomy@gmail.com

MATERIALS AND METHODS

Early tadpoles of *Bufo regularis and Bufo viridis* (family *Bufonidae), Rana bedriagae* and *Ptychadena mascareniesis* (family *Ranidae*) (Marx, 1968) were used in the present study. *Bufo regularis, Rana bedriagae and Phychadena mascareniesis* were collected from the ponds of Abou Rawash, Giza Governorate, Egypt, while *Bufo viridis* was collected from Alexandria, Egypt. During the breeding season, which lasts from March to about the end of October, the tadpoles were reared in glass aquaria (60 x 30 x 30cm) at room temperature 27°c ± 2°c in the laboratory of Department of Zoology, Faculty of Science, University of Cairo. The glass aquaria were provided with a sufficient supply of Dechlorinated tap water. Dechlorination was carried out by leaving the ordinary tap water in large aquaria in an aerated place, at least for one day. During the aquatic period of the animal's life, dechlorniated tap water was exclusively used as a rearing medium throughout the study. The water medium was changed every third day and provided with water plants.

Four embryonic stages were selected for this study. Staging of the individuals was typed according to the Normal Table of Development (Gosner, 1960; Sedra and Michael, 1961). The selected stages were numbered 54-58, 59-61, 62-63 and 64-66. Tadpoles were reared in petri-dishes with dechlorniated tap water until they reached the required stage. A total of 1600 tadpoles were used in the present study (at least 400 for each species). Tadpoles were randomly divided into groups and preserved according to the experimental demands. The age, length and body weight parameters were used to define the larval stages according to Abu-Tira *et al*., (2005 a,b) and Saad *et al*., (2005). Moribund embryos were continuously removed from the culture. Embryos from several different parents were used to ensure that the results are not continued to a particular batch. All animal experiments were approved by the University Animal Experimental Ethics Committee, and were in accordance with the guidelines of the Committee for the Purpose of Control and Supervision of Experiments on Animal (CPCSEA), Government of Egypt.

The livers of the tested tadpoles were fixed in aqueous Bouin's solution at room temperature for 24h, dehydrated through serial dilutions of ethanol and finally embedded in paraffin wax. Transverse sections of a thickness of 7 microns were serially cut. Sections were stained with heamatoxylin and eosin. The slides were examined in Niken Diapho TMD micro-scope.

The livers of the tested tadpoles were fixed overnight in 2.5% glutaraldhyde at pH 7.4 in 0.1 M sodium cocodylate buffer at 4°C. The fragments were post-fixed with 1% OsO4 for two hours, dehydrated in agraded series of ethanol and embedded in resin (TAAB, Aldermaston, UK). Ultrathin sections, obtained with a LKB ultratome III, were stained with uranyl acetate and lead citrate ,and examined in a Zeiss EM 10C electron microscopy.

In apoptotic cells, specific DNA cleavage becomes evident in electrophoresis analysis as a typical pattern due to multiple DNA fragments (Aaij and Borst, 1972; Compton, 1992; Hale *et al*., 1996). 0.5 ml of cell suspension (cell suspension at 1-5×10^6 cells/ml in complete RPMI medium which consists of 5% heat-inactivated fetal calf serum (FCS), 2 mM L-glutamine, 25mM HEPES buffer, 50µg/ml gentamicin sulfate) in tubes labeled B. Centrifuge cells at 200×g at 4°C for 10 min. Than supernatants were carefully transferred in new tubes labeled S. 0.5 ml of TTE solution (TE buffer (10 mM Tris.Cl pH 7.4, 1 mM EDTA) was added with 0.2% Triton x-100 (store at 4ºC)) in tubes B and was vortexed vigorously, tubes B were centrifuged at 20,000×g for 10 min at 4ºC, Then super-natants were carefully transferred in new tubes labeled T (top), 0.5 ml of TTE solution in tubes B was added, together with 0.1 ml of ice–cold 5M NaCl to the 0.5 ml volume present in tubes B and T and were vortexed vigorously. 0.7 ml of ice–cold isopropanol was added to each tube and were vortexed vigorously, Then the tubes were leaved overnight at -20ºC. For precipitation, DNA was recovered by pelleting for 10 min at 20,000×g at 4ºC, the supernatants were discarded. For elution of DNA, 0.5-0.7 ml ice –cold 70% ethanol was added to each tube, then the tubes were centrifuged at 20,000×g for 10 min at 4ºC, the supernatants were discarded, 20-50µl TTE solution was added to each tube, then the tubes were placed at 37°C for 1-3 days. For sample preparation, 10× loading buffer were mixed with the samples of DNA to final concentration of 1×. Additionally, a DNA molecular weight marker was prepared by mixing with loading buffer. The samples were placed in a heating block at 65º C for 10 min and immediately 7 µl of them were loaded to each well of standard 1% agarose gel containing ethidium bromide 0.5 mg/ml. Appropriate DNA markers were used. The electrophoresis was run in standard TBE buffer after setting the voltage to 75 V. The power supply was turned off when bromophenol blue dye from the loading buffer has migrated to the end of the platform. To visualize DNA, the gel was placed on a UV transilluminator and photographed.

RESULTS AND DISCUSSION

Embryonic stages:

The developmental stage of *Bufo regularis* and *Bufo viridis* was determined using the staging system developed for pelobatid frogs by Gosner (1960) and of *Rana bedriagae* tadpoles using the Taylor-Kollors (1946) staging system developed for ranid frogs. The term of Etkin (1968) which describes the general stages of amphibian development, premetamorphosis (early larval stage which precedes hind limb development), pro-metamorphosis (period of rapid hind limb development) and climax (front limb emergence and other dramatic morphologic changes) are also used. D'Angelo *et al*. (1941) showed that once ranid frog tadpoles reach a critical point in development, which they defined based on hind limb length, inanition accelerate metamorphosis. As the larval period of *R. catesbeiana* tadpoles is highly variable and can range from several months to years (Denver, 1993), were choosen to create conditions which would favour metamor-phosis. Thus, we used the developmental criteria of D'Angelo *et al*. (1941) in designing our experiments with the *Ptychadena mascareniesis* larval development of the four tested species are summarized in Table (1).

Table 1: Larval development of *Bufo regularis, Bufo viridis, Rana bedriagae* and *Ptychadena mascareniesis* in 10% seawater (water temperature 28°C):

Stage	Time after fertilization (days)*	Total length	Notes***
Prometamorphosis (st. 54 to 58)	20	17.0	- limb bud become visible - horny teeth fully developed - pigmentation evident on abdomen
Beginning of climax (st. 54 to 61)	30-50	33.0-45.0	- five toes distinct - toe pads appear - hind limb elongate
Middle of climax (st. 62 to 63)	50	26.0- 32.0	- forelimbs appear - tail fins absorbed - tail shorter than hind limb
End of climax (st. 64 to 66)	43-44	13.0	- stub of tail remains - metamorphosis accomplished

* Individual variation in the progress of development was large.
** Total length is defined as the length from tip of snout to tip of the tail and to vent in tadpole and frog or toad, respectively.
*** Number of animals used for measurement was 5-10.

Light Microscopical Study:

In the present study, we observed a close correspondence between the morphology of light microscopy in this study and pyknotic cells in standard histological section (Kerr *et al*., 1972). As shown in Figs. (1-4) in the dissected section of the four tested species of anuran amphibians during development, the nuclei of apoptotic cells were brown-black masses and were either rounded or shrunken (pyknotic). All embryonic stages described in the present study contained apoptotic cells with both rounded and shrunken morphologies. The dynamics of liver apoptosis in the four tested species of anuran amphibians generally followed the time course described in other organisms (Saad and El-Masri, 1995; Abu-Tira *et al*., 2005a,b; Saad *et al*., 2005). Previous studies have described a rapid rate of dead cell clearance with cells being removed in 2 h or less (Saad *et al*., 2005). In the present study, comparison of the tail bud in embryos at 2h intervals suggested that apoptotic cells in this region were completely eliminated within 8 h. The large numbers of apoptotic cells observed in prometamorphosis were absent in the end of climax. This rapid apoptotic clearance in the tested species is a limiting factor in our study. Apoptotic cells in the liver could be readily determined by their distinctive apoptotic appearance. H-E staining revealed that the apoptotic hepatic cells shrunk, leaving a gap with cell borders, and they featured pyknotic nuclei and condensed chromatin, recognizable as apoptotic bodies in Figs. (1-4).

Electron Microscopical Study:

To determine whether the ultra-structural morphology of embryonic cell death is characteristic of apoptosis (Kerr *et al*., 1995), sections from prometamorphosis until the end of climax were examined in the four tested species of anuran amphibians by electron microscopy. During prometamorphosis (Stage 54 to 58), the chromatin was condensed and aggregated in sharply delineated, uniformly dense masses, which in some cases were seen to about the inner surface of the nuclear membrane. The nuclear membrane was clearly intact, as were the cellular membranes. Budding of the nucleus to produce discrete nuclear fragments of varying size and chromatin content, which are still surrounded by double membranes, was also detected. Organelles remain well preserved and the mitochondria are clearly identifiable at this time. (Figs. 5A, 6A, 7A and 8A).

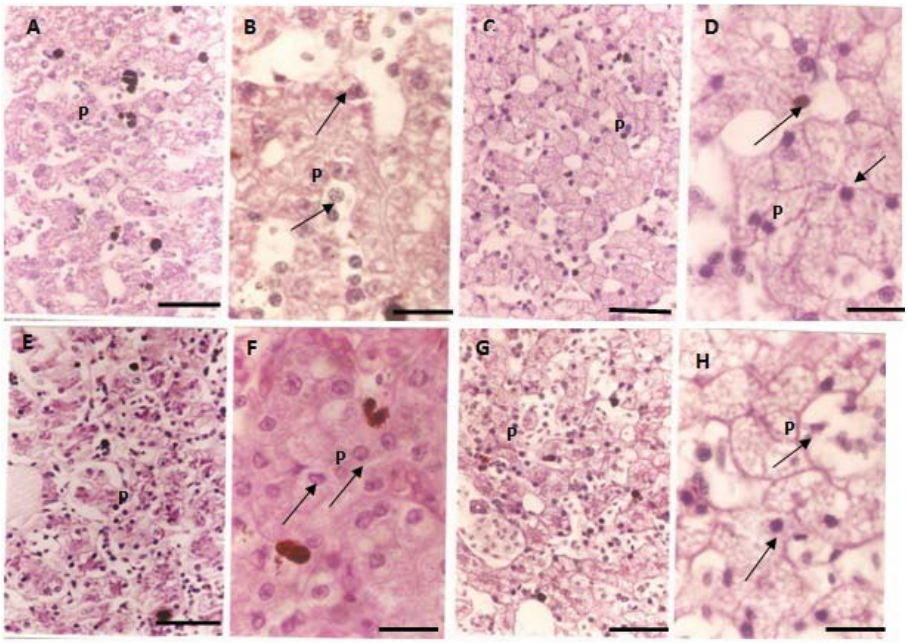

Fig. 1: Histological sections of liver of *Bufo regularis*. (A) (B) at prometamorphosis (stage 54 to 58). (C) (D) beginning of climax (stage 59 to 61). (E) (F) middle of climax (stage 62 to 63). (G) (H) end of climax (stage 64 to 66). Apoptotic cells (arrows) occur mainly around blood vessels. Dark pigment granules are scattered in the liver (P) Bar, 25.

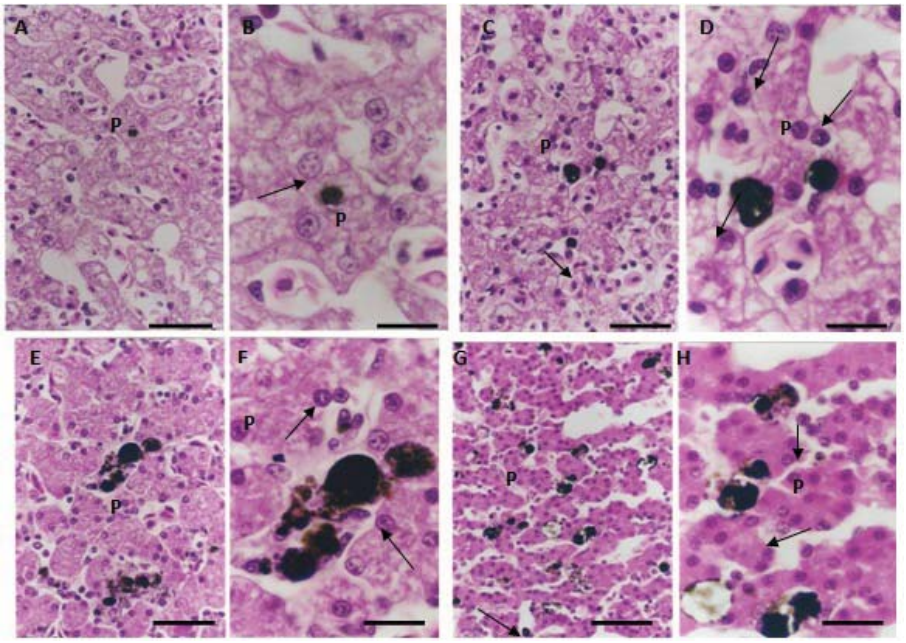

Fig. 2: Histological sections of liver of *Bufo viridis*. (A) (B) at prometamorphosis (stage 54 to 58). (C) (D) beginning of climax (stage 59 to 61). (E) (F) middle of climax (stage 62 to 63). (G) (H) end of climax (stage 64 to 66). A large number of apoptotic cells (arrows) occurs. Dark pigment granules are scattered in the liver (P). Bar, 25.

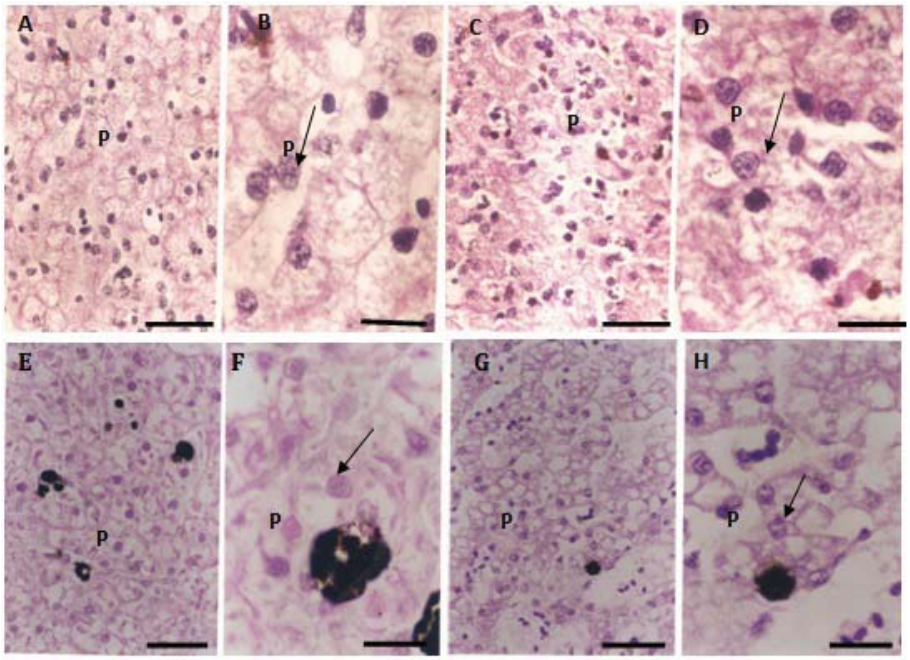

Fig. 3: Histological sections of liver of *Rana bedriagae*. (A) (B) at prometamorphosis (stage 54 to 58). (C) (D) beginning of climax (stage 59 to 61). (E) (F) middle of climax (stage 62 to 63). (G) (H) end of climax (stage 64 to 66). Apoptotic cells (arrows) are localized mainly in the parenchymatous tissue. Dark pigment granules are scattered in the liver (P). Bar, 25.

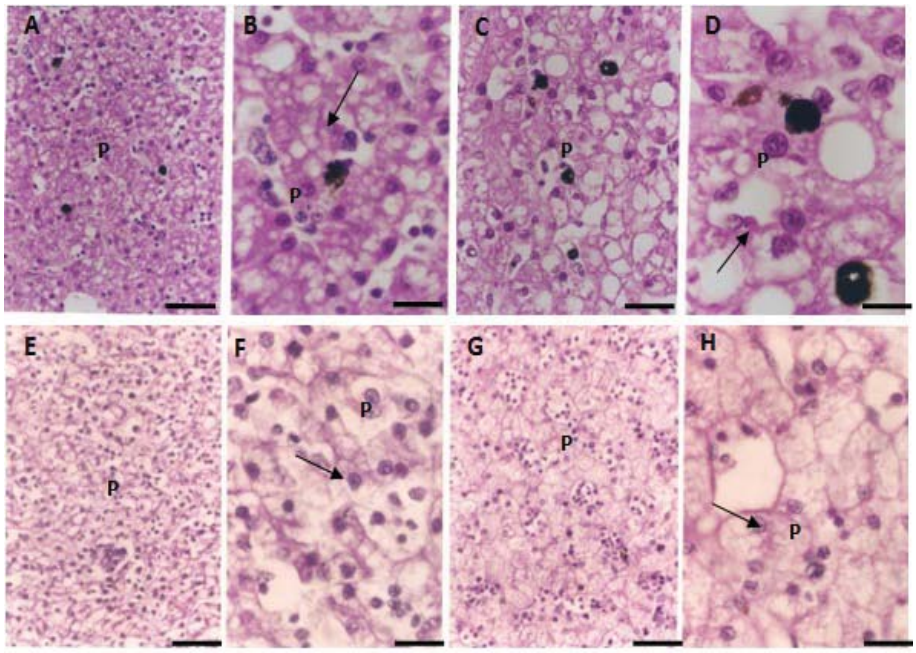

Fig. 4: Histological sections of liver of *Ptychadena mascareniesis*. (A) (B) at prometamorphosis (stage 54 to 58). (C) (D) beginning of climax (stage 59 to 61). (E) (F) middle of climax (stage 62 to 63). (G) (H) end of climax (stage 64 to 66). Apoptotic cells (arrows) are few. They are localized mainly around blood vessels. Dark pigments granules are scattered in the liver (P). Bar, 25

At the beginning of climax (stage 59 to 61), the liver parenchyma consisted of large hepatocytes arranged in laminae of two cell thick, separating adjacent sinusoids. All the hepatocytes showed a polarity of intracellular components. The cytoplasm of all hepatocytes was filled for the most part with glycogen, so that few organelles present in the cells (mitochondria, rough endoplasmic reticulum and lysosomes) were suggested in a restricted peribiliar area or encircling the cell nucleus (Figs. 5B, 6B, 7B and 8B).

At the middle of climax (stage 62 to 63), the general organization of liver tissue was similar to that previously described, but with major morphological differences between the beginning and the middle of climax hepatocytes. Hepatocellular volume was reduced, presumably an effect linked to the dramatic depletion of glycogen content. The polar localization of organelles was no longer evident in these stages. Variable numbers of mitochondria were scattered throughout the cytoplasm, in greater numbers and larger than those of previous stages, although no measurements were made. The cisternae of the rough endoplasmic reticulum (RER) were in parallel arrays, sometimes in close association with the mitochondria; in some cells the RER was slightly dilated (Figs. 5C, 6C, 7C and 8C).

At the end of climax (stages 64 to 66), the hepatocytes exhibited a specific morphological aspect: Hepatocellular volume was increased because of the large and very dense glycogen field. However, inspite of the abundance of glycogen, numerous organelles were still scattered throughout the cytoplasm. The mito-chondria were very numerous, but small in size and with a rather dense matrix. There were numerous stacks of parallel cisternae of RER both throughout the cytoplasm and in proximity to the nucleus. A few lipid droplets were observed at the periphery of most cells (Figs. 5D, 6D, 7D and 8D). These features are typical of apoptotic cells were observed in the four anuran species during embryogenesis till the end of climax.

Electron Microscopical Study:

To determine whether the ultra-structural morphology of embryonic cell death is characteristic of apoptosis (Kerr *et al*., '95), sections from prometamorphosis until the end of climax were examined in the four tested species of anuran amphibians by electron microscopy. During prometamorphosis (Stage 54 to 58), the chromatin was condensed and aggregated in sharply delineated, uniformly dense masses, which in some cases were seen to about the inner surface of the nuclear membrane. The nuclear membrane was clearly intact, as were the cellular membranes. Budding of the nucleus to produce discrete nuclear fragments of varying size and chromatin content, which are still surrounded by double membranes, was also detected. Organelles remain well preserved and the mitochondria are clearly identifiable at this time. (Figs. 5A, 6A, 7A and 8A).

At the beginning of climax (stage 59 to 61), the liver parenchyma consisted of large hepatocytes arranged in laminae of two cell thick, separating adjacent sinusoids. All the hepatocytes showed a polarity of intracellular components. The cytoplasm of all hepatocytes was filled for the most part with glycogen, so that few organelles present in the cells (mitochondria, rough endoplasmic reticulum and lysosomes) were suggested in a restricted peribiliar area or encircling the cell nucleus (Figs. 5B, 6B, 7B and 8B).

At the middle of climax (stage 62 to 63), the general organization of liver tissue was similar to that previously described, but with major morphological differences between the beginning and the middle of climax hepato-cytes. Hepatocellular volume was reduced, presumably an effect linked to the dramatic depletion of glycogen content. The polar localization of organelles was no longer evident in these stages. Variable numbers of mitochondria were scattered throughout the cytoplasm, in greater numbers and larger than those of previous stages, although no measurements were made. The cisternae of the rough endoplasmic reticulum (RER) were in parallel arrays, sometimes in close association with the mitochondria; in some cells the RER was slightly dilated (Figs. 5C, 6C, 7C and 8C).

At the end of climax (stages 64 to 66), the hepatocytes exhibited a specific morphological aspect: Hepatocellular volume was increased because of the large and very dense glycogen field. However, inspite of the abundance of glycogen, numerous organelles were still scattered throughout the cytoplasm. The mito-chondria were very numerous, but small in size and with a rather dense matrix. There were numerous stacks of parallel cisternae of RER both throughout the cytoplasm and in proximity to the nucleus. A few lipid droplets were observed at the periphery of most cells (Figs. 5D, 6D, 7D and 8D). These features are typical of apoptotic cells were observed in the four anuran species during embryogenesis till the end of climax.

Biochemical Characterization of Liver Apoptosis:

To confirm the morphological signs of apoptosis, we performed DNA electro-phoresis which is the technique used to characterize apoptosis biochemically. The multimeter fragments ladders characteristic of the apoptotic process were compared with the molecular size marker in base pair, as indicated in lane M (Fig. 9). The analysis of DNA fragmentation by conventional agarose gel electrophoresis revealed a ladder of DNA fragments in multiple of 180 bp in length, pointing to an internucleosomal DNA cleavage. When pulsed-field gel electrophoresis was performed on liver cells from the four tested species of anuran amphibians, the electro-phoretic pattern indicated the formation of high Mol.Wt. Fragments ranging from 1.5 Mb to 73 Kb in length. Strong and weak smears of high Mol.Wt. DNA could be observed in all samples (Fig. 9).

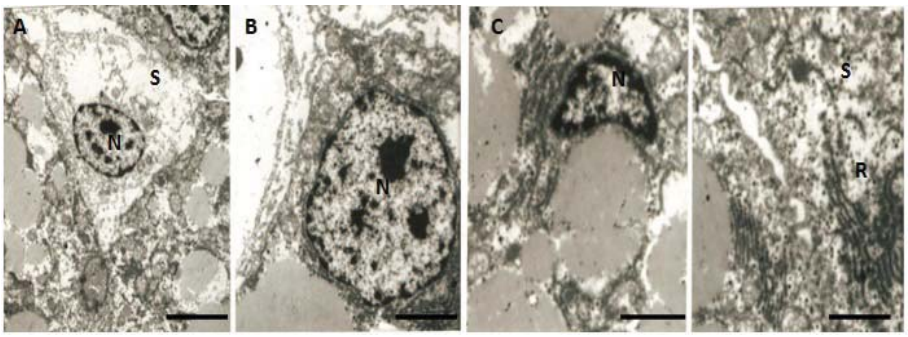

Fig. 5: Electron micrograph reveals morphological features typical of apoptotic cells in the liver of *Bufo regularis*. (A) at prometamorphosis (stage 54 to 58) (B) beginning of climax (stage 59 to 61) (C) middle of climax (stage 62 to 63) (D) end of climax (stage 64 to 66). Apoptotic body with crescent-shaped nucleus (N) and dark cytoplasm surrounded by a large intercellular space (S). RER (R) appear intact. Bar, 25

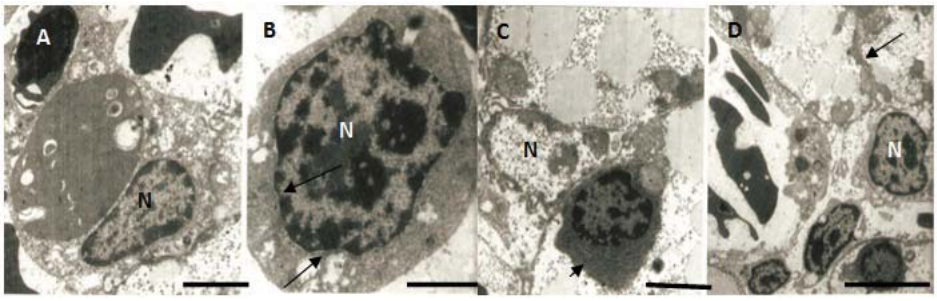

Fig. 6: Electron micrograph reveals morphological features typical of apoptotic cells in the liver of *Bufo viridis*. (A) at prometamorphosis (stage 54 to 58) (B) beginning of climax (stage 59 to 61) (C) middle of climax (stage 62 to 63) (D) end of climax (stage 64 to 66). Apoptotic body containing autophagic vacuoles (arrows). Hepatic cell shows dark cytoplasm and digitations of the cell membrane (head arrow). The nucleus (N) is unaffected. Bar, 25.

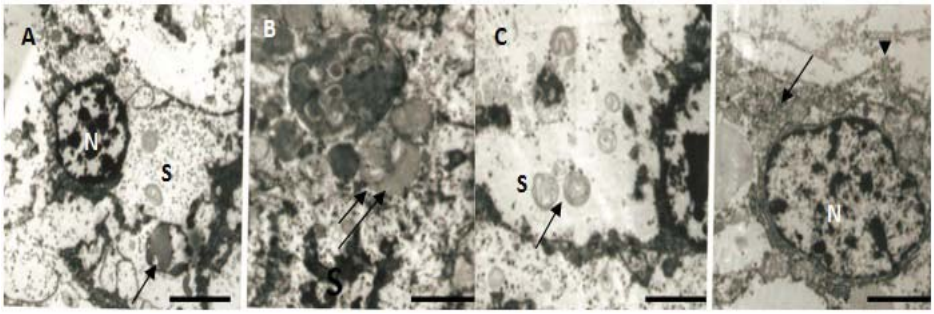

Fig. 7: Electron micrograph reveals morphological features typical of apoptotic cells in the liver of *Rana bedriagae*. (A) at prometamorphosis (stage 54 to 58) (B) beginning of climax (stage 59 to 61) (C) middle of climax (stage 62 to 63) (D) end of climax (stage 64 to 66). Apoptotic cells containing dark secretory granules (arrows). The nuclei of apoptotic cells (N) show condensed chromatin. Cytoplasmic projections (head arrow) extend in large intercellular spaces (S). Bar, 25

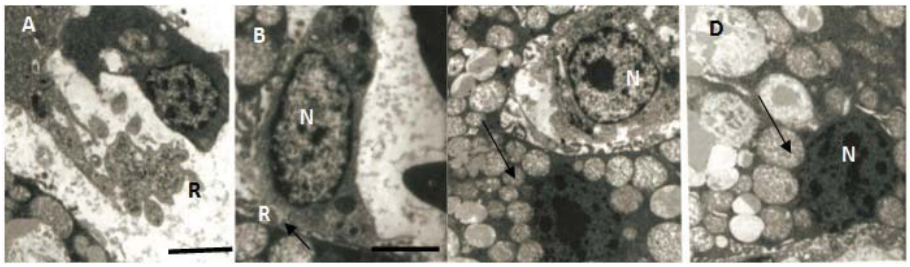

Fig. 8: Electron micrograph reveals morphological features typical of apoptotic cells in the liver of *Ptychadena mascareniesis*. (A) at prometamorphosis (stage 54 to 58) (B) beginning of climax (stage 59 to 61) (C) middle of climax (stage 62 to 63) (D) end of climax (stage 64 to 66). Hepatic cells are arranged in acini, have a pyramidal shape and contain large amount of RER (R) and secretory granules (arrow). The nuclei (N) of hepatic cells show condensed chromatin. Bar, 25

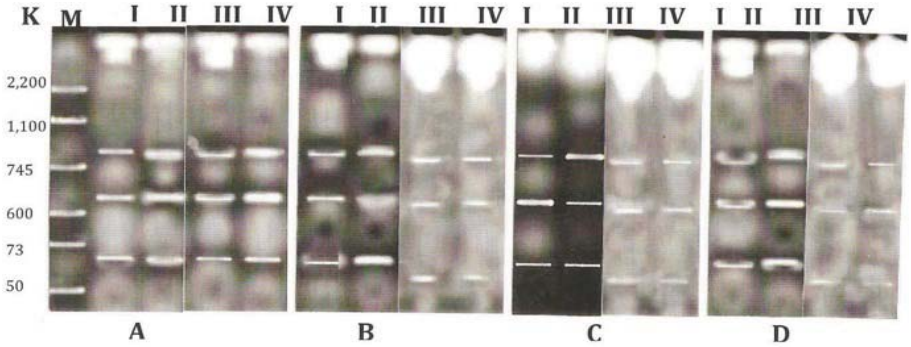

Fig. 9: Agarose gel electrophoresis of liver DNA of *Bufo regularis* (A), *Bufo viridis* (B), *Rana bedriagae* (C) and *Ptychadena mascareniesis* (D). Reference MW markers are shown in lane M. Different stages of metamorphosis are given in the top of the figure. I: Prometamorphosis (stage 54 to 58), II: Beginning of climax (stage 54 to 61), III: Middle of climax (stage 62 to 63); IV: End of climax (stage 64 to 66).

Discussion:

Deletion of hepatic cells during embryonic development and spontaneous metamorphosis of the four tested species of anuran amphibians is accomplished by ultrastructurally typical apoptosis; the morphological appearance being essentially the same as those described in vertebrate embryos (Glucksmann , 1951; Bellairs, 1961; Farbman, 1968; Manasek, 1969; Webster and Gross, 1970; Mottet and Hammar, 1972).The phenomenon involves a stereo typed sequence of changes ,and begins with peripheral aggregation of nuclear chromatin; This is followed by nuclear fragmentation and cytoplasmic condensation associated with prolific budding to produce membrane–bound apoptotic bodies of varying sizes. As is the case in other solid tissues, the actual processes of budding is rarely observed, possibly viable cells engulf the condensing ones (Kerr, 1973; Kornbluth and Evans, 2001; Tsuchiya *et al*., 2005; Saelim *et al*., 2007; Hasebe *et al*., 2007).

A few of the apoptotic bodies in the amphibians liver are ingested by liver kupffer cells. However, the paucity of secondary lysosomes in these cells at a fairly advanced stage of embryogenesis suggests that they play a relatively minor role in disposing of fragments. Hepatic macrophages and kupffer cells are sometimes more active in this regard during embryonic development (Tsuchiya *et al*., 2005; Fujimoto *et al*., 2007; Menon and Rozman, 2007). The majority of the bodies in the liver are ingested and degraded by specialized cells, whose cytoplasm becomes progressively laden with telo-lysosomes.

In an electron microscopical study of the liver changes in thyroxine–induced organ involution carried out by Gupta *et al*. (2008), a clear distinction was not made between autophagy on the one hand and heterophagy of the cell remnants on the other. Autophagic vacuoles may indeed be difficult to distinguish from ingested apoptotic bodies that do not contain nuclear remnants (Hasebe *et al*., 2007; Taniguchi *et al*., 2008). However, differentiation between these two processes is important, for the former merely involves segregation and degrading of part of the cytoplasm of a viable cell, while the latter is an indication of cell death. Autophagy undoubtedly occurs in the embryonic liver (Ishizuya-Oka and Shi, 2005; Furlow and Neff, 2006; Hogan *et al*., 2007), but our findings do not suggest that it plays a major part in the regressive process.

Programmed cell death (apoptosis) in anuran amphibian embryos starts at the onset of gastrulation and then continues during gastrulation and neurulation (Hensey and Gautier, 1998). During these early stages, apoptosis seems to occur without obvious peaks in time or space. In contrast, during the stages we analyzed in the present study, the frequency of cell death was high variable depending on the developmental stage and the species of anuran amphibians used. Furthermore, apoptosis occurred in some species as a single wave; whereas at least two distinct waves could be detected in other species.

The first large wave was observed at prometamorphosis. Several species (*B. regularis, B. viridis and P. mascareniesis*) presented apoptotic cells in the liver. Sub-stantial cell death was also observed in *R. bedriagae.* During these phases, which seem to constitute a critical choice-point for survival, the tadpoles were very sensitive to temperature and feeding conditions (Buchholz and Hayes, 2005; Menon and Rozman, 2007). There is perhaps a causal link between the extensive remodeling of vital organs and this high fragility. During the subsequent growth period, i.e., the beginning of climax, no massive cell death occurred. However, some apoptotic cells could be observed by electron microscopy in the liver of *B. regularis* and *B. viridis.* The second wave of apoptosis was observed during metamorphosis, particularly during the end of climax. The cell death concerned essentially the liver of *B. regularis* and B. *viridis* and to less extent the liver of *R. bedriagae* and *P. mascareniesis.*

Metamorphosis is a highly complex series of events controlled by thyroid hormones (Sachs *et al*., 2000), the Bcl-X (L) homologue (Coen *et al*., 2001), caspases (Nakajima *et al*., 2000) and other factors. In the present study, we were interested in knowing how, and to what extent, the timing of liver apoptosis is correlated with that of tail degeneration and forelimb/hind limb development. Although many of the stained cells displayed clearly hepatic cell morphology, it is difficult to evaluate the ratio between degenerating hepatic versus non-hepatic cells, since the duration of apoptosis, and therefore the chance to detect apoptotic cells prior to their disappearance may be different.

During metamorphosis and particularly the climax, severe cell death could be observed in the liver of the tested anuran species. Interestingly, cell death of cells, started before the tail resportion, and it was observable over a long period. From stage 58 (beginning of climax and tail regression), cell death in the liver was increasingly observed in the liver. In agreement with Estabel *et al*., (2003), we found heavy cell death affecting the liver prior to climax (stages 54 to 58). This observation fits with studies of hepatic resident macrophage activity (Purrello *et al*., 2001; Frangioni *et al*., 2005; Koibuchi *et al*., 2008). Macrophages initially appeared at early climax, increased rapidly in number during muscle regression, and reach peak density at late climax (Nishikawa *et al*., 1998; Hensey and Gautier, 1998; Zorn and Mason, 2001; Szalewicz *et al*., 2003; Frangioni *et al*., 2006).

The present study demonstrates that liver histogenesis took place mostly by means of programmed cell death (PCD). This process began at the end of prometamorphosis (around stage 58, after the accomplishment of hind limb differentiation), and continued throughout the metamorphic climax (stages 59-63), characterized by fore limb emission and by tail resorption. In this period the tadpoles of the tested species of anura circular patches of apoptotic cells could originate from a single damaged cell and it is likely that some embryos would have more damaged cells than other, thus explaining some of the variation in amount of cell death is observed. In addition, cell death at this time could also be the consequence of the mechanical stress that cells subjected to at this stage. In the same period, mechanical stress due to neuroectodermal cells movement occurred as demonstrated by Cheng *et al.* (1995) and Hensey and Gautier (1998) in *X. laevis*.

The number of apoptotic cells in the liver was particularly high during the period from the end of prometamorphosis, during which hind limb differentiated to the metamorphic climax, when fore limb emission and tail resorption occurred. Apoptotic cells were mostly localized around blood vessels and hepatic acini. This localization suggests that the input to start the process of PCD arrived via information transmitted through the circulatory system. PCD is considered to be under genetic control (Das *et al*., 2006; Page *et al*., 2008), but is also possible that hormonal information is responsible for its induction, like thyroxine in the degeneration of tadpole tail (Phillips and Platt, 1994; Assisi *et al*., 1999; Bratosin *et al*., 2004; Veldhoen *et al*., 2006; Shi *et al*., 2007).

The features described in the liver cells of the four tested species of anuran amphibians during metamorphic climax are characteristic of the so- called heterophagic cell death or apoptosis, and have been described with similar patterns in many degenerating issues of vertebrate and invertebrates (Wyllie *et al*., 1980; Clarke, 1990; Kerr *et al*., 1995; Sanders and Wride, 1995). The most common features are nuclear convolution with chromatin conden-sation and cell membrane protrusions. The cytoplasm appears rather dense, sometimes vacuolated, and organelles such as RER and mitochondria are intact. One interesting aspect of apoptosis is that its morphological characteristics appear to be constant throughout the phylogenetic tree.

It is widely believed that the apoptotic process is very short. According to Sanders and Wride (1995), DNA fragmentation precedes the morphological changes visible in apoptotic cells. Conversely, Collins *et al*. (1997) claimed that nuclear condensation occurrs before DNA fragmentation. As for the elimination of dead cells is concerned, many authors suggest that cells are phagocytosed by macrophages and by normal mesenchymal cells which become phagocytic (Shook *et al*., 2004; Johnston *et al*., 2005; Vignal *et al*., 2007). Our observations show the occasional presence of macrophages among apoptotic cells. They have a lobed nucleus, dark cytoplasm and long projections which surround the apoptotic bodies.

REFERENCES

Aaji, C., P. Borst, 1972. Gel-electrophoresis of DNA. Biochimica ET Biophysica Acta, 269(2): 192-198.

Abu-Taira, A., F. EI-Badry, A.H. Saad, 2005a. Embryonic development of heteroploid *Bufo regularis* (Amphibia, Bufonidae) I. Histogenesis of the lymphoid organs. Egypt. J. Zool., 45: 1-29.

Abu-Taira, A., F. EI-Badry, A.H. Saad, 2005b. Embryonic development of heteroploid *Bufo regularis* (Amphibia, Bufonidae) II. Development of the gut. Egypt. J. Zool., 45: 31-54.

Amphibia Web, http:// elib. cs. berkeley. Edu /aw/,access date Dec. 3: 2004.

Arends, M.J., A.H. Wyllie, 1991. Apoptosis. Mechanism and role in pathology. Int. Rev. Exp. Pathol., 32: 223-254.

Assisi, L., F. Autuori, V. Botte, M.G. Farrace, M. Piacentini 1999. Hormonal control of tissue transglutaminase indution during programmed cell death in frog liver. Exp. Cell Res., 247: 339-346.

Bellairs, R., 1961. Cell death in chick embryos as studied by electron microscopy. J. Anat. 95: 54-60.

Bratosin, D., Estaquier, J., Slomianny, C., Tissier, J.P., B. Quatannens, T. Bulai, L. Mitrofan, A. Marinescu, L.Trandaburu, J.C. Ameisen, J. Montreuil, 2004. On the evolution of erythrocyte programmed cell death apoptosis of *Rana esculenta* nucleated red blood cells involves cysteine proteinase activation and mitochondrion permeabili-zation. Biochimie., 86(3): 183-92.

Buchholz, D.R., T.B. Hayes, 2005. Variation in thyroid hormone action and tissue content underlies species differences in the timing of metamorphosis in desert frogs. Evol. Dev., (5): 458-67.

Cheng, W., L. Baosheng, G. Kajstura, P. Li, M.S. Wolin, E.H. Sonnenblick, T.H. Hintze, G. Olivetti, P. Anversa 1995. Stretch-induced programmed cell diversity J. Clin. Invest., 96: 2247-2259.

Clarke, P.G.H., 1990. Developmental cell Death: morphological Diversity and multiple Mechanisms. Anatomy and Embryology, 181: 195-213.

Coen, L., D. Du Pasquier, S. Le Mevel, S. Brown, J. Tata, A. Mazabraud, B.A. Demeneix, 2001. *Xenopus* Bcl-XL selectively protects Rohon-Beard neurons from metamorphic degeneration. Proc. Natl. Acad. Sci. USA, 98: 7869-7874.

Compton, M.M., 1992. Abiochemical hallmark of apoptosis: internucleosomal degradation of the genome. Cancer Metastesis, 11: 105-19.

D'Angelo, S.A., A.S. Gordon, H.A. Charipper, 1941. The role of the thyroid and pituitary glands in the anomalous effect of inanition on amphibian metamorphosis. J. Exp. Zool., 87: 259-277.

Das, B., L. Cai, M.G. Carter, Y.L. Piao A.A. Sharov, M.S.H. Ko, D.D. Brown, 2006. Gene expression changes at metamorphosis induced by thyroid hormone in *Xenopus laevis* tadpoles. Dev. Biol., 291: 342-355.

Denver, R.J., 1993. Acceleration of anuran amphibian metamorphosis by corticotropin-releasing-hormonelike peptides. Gen Comp Endocrinol., 91(1): 38-51.

Estabel, J., A. Mercer, N. Konig, J. Exbrayat, 2003. Programmed cell death in *Xenopus laevis* spinal cord, tail and other tissues, prior to, and during, metamorphosis Life Sciences, 73: 3297-3306.

Etkin, W.B., 1968. Hormonal control of amphibian metamorphosis. In: Metamorphosis-A Problem in Developmental Biology. W. Etkin and L. Gilbert, eds. Appleton-Century-Crofts, New York, pp: 313-348.

Farbman, A.I., 1968. Electron microscope study of palate fusion in mouse embryos. Dev. Biol., 18: 93-116.

Frangioni, G., M. Santoni, S. Bianchi, M. Franchi, G. Fuzzi, S.Marcaccini, C. Varlani, G. Borgioli, 2005. Function of hepatic melanogenesis in the newt. *Triturus carnifex*. J. Exp. Zool., A. 303: 123-131.

Frangioni, G., A.Atzori, M. Balzi, G. Fuzzi, A. Ghinassi, N. Pescosolido, S. Bianchi, G. Borgioli, 2006. Thyroid and hypoxic stress in the newt, *Carnifex*. J. of Exp. Zool., 305A: 225-232.

Fujimoto, K., K. Nakajima, Y. Yaoita, 2007. Expression of matrix metalloproteinase genes in regressing or remodeling organs during amphibian metamorphosis. Dev. Growth Differ., (2): 131-43.

Furlow, J.D., E.S. Neff, 2006. A developmental switch induced by thyroid hormone: *Xenopus laevis* metamorphosis. Trends Endocrinol. Metab., 17: 40-47.

Glucksmann, A., 1951. Cell deaths in normal vertebrate ontogeny. Biol. Rev., 26: 59-86.

Gosner, K.L., 1960. A simplified table for staging anuran embryos and larvae with notes on identification. Herpetologica, 16: 183-190.

Gupta, N., A. Hitchings, L. Weber, M. Wickstrom 2008. Two novel biomarkers in developing wood frogs. Integr. Environ. Assess Manag., (l): 129-30.

Hale, A.J., C.A. Smith, L.C. Sutherland, V.E.A. Stoneman, V.L. Longthorne, A.C. Culhane, G.T. Williams 1996. Apoptosis: Molecular regulation of cell death. Eur. J. Biochem., 236:1-26.

Hasebe, T., M. Kajita,, K. Fujimoto, Y. Yaoita, A. Ishizuya-Oka, 2007. Expression profiles of the duplicated matrix metallo-proteinase-9 genes suggest their different roles in apoptosis of larval intestinal epithelial cells during *Xenopus laevis* metamorphosis. Dev. Dyn., (8): 2338-45.

Hensey, C., J. Gautier, 1998. Programmed cell death during *Xenopus* development: a spatio-temporal analysis. Dev. Biol., 203: 36-48.

Hogan, N.S., K.L. Crump, P. Duarte, D.R. Lean, V.L. Trudeau 2007. Hormone cross-regulation in the tadpole brain: develop-pmental expression profiles and effect of T3 exposure on thyroid hormone- and estrogen-responsive genes in *Rana pipiens*. Gen. Comp. Endocrinol., (1-3): 5-15.

Ishizuya-Oka, A., Y.B. Shi, 2005. Molecular mechanisms for thyroid hormone-induced remodeling in the amphibian digestive tract: a model for studying organ regeneration. Dev. Growth Differ., 47(9): 601-7.

Johnston, J., R. Chan, M. Calderon-Segura, S. McFarlane, L.W. Browder 2005. The roles of BcI-xl in modulating apoptosis during development of *Xenopus laevis*. BMC Development Biology, 5: 20.

Kerr, J.F.R., 1973. Some lysosome functions in liver cells reacting to sublethal injury. In Lysosomes in Biology and Pathology, vol. 3 (ed. J.T. Dingle), pp. 365-394. Amsterdam and London: North-Holland.

Kerr, J.F.R., A.H. A.R. WyllieCurrie 1972. Apoptosis: a basic biological phenomenon with wide-ranging imply-cations in tissue kinetics. Br. J. Cancer, 26: 239-257.

Kerr, J.F.R., E.G.C Gob, C.M. Winterford, B.V. Harmon, 1995. Anatomical methods in cell death. Methods in Cell Biology, 46: 1-27.

Kloc, M., Y. Shirato, S. Bilinski, L.W. Browder, J. Johnston 2007. Differential subcellular sequestration of proapoptotic and anti-apoptotic proteins and colocali-zation of Bcl-x (L) with the germ plasm in *Xenopus laevis* oocytes. Genesis., 45(8): 523-31.

Knapp, D., N. Messenger, A. Ahmed Rana, Smith, J.C., 2006. Neurotrophin receptor homolog (NRH1) proteins regulate mesoderm formation and apoptosis during early *Xenopus* development. Dev. Biol., (2):554-69.

Koibuchi, N., Y. Kaneda, Y. Taniyama, K. Matsumoto, T. Nakamura, T. Ogihara, R. Morishita 2008. Essential role of HGF (hepatocyte growth factor) in blood formation in *Xenopus*. Blood., 103(9): 3320-3325.

Kornbluth, S., E.K. Evans, 2001. Analysis of apoptosis using *Xenopus* egg extracts. Curr. Protoc. Cell Biol., Chapter 11: Unit., 11: 12.

Manasek, F.J., 1969. Myocardial cell death in the embryonic chick ventricle. J. Embryol. Exp. Morph., 21: 271-284.

Marx, H., 1968. Check list of the reptiles and amphibians of Egypt. Spec. Res. Unit. No. 3.

Menon, J., R.Rozman, 2007. Oxidative stress, tissue remodeling and regression during amphibian metamorphosis. Comp. Biochem. Physiol. C. Toxicol. Pharmacol.., (4): 625-31.

Mottet, N.K., S.P. Hammar, 1972. Ribosome crystals in necrotizing cells from the posterior necrotic zone of the developing chick limb. Cell Sci., 11: 403-414.

Nakajima, K., A. Takahashi, Y. Yaoita, 2000. Structure, expression, and function of *Xenopus laevis* caspase family. J. Biol. Chem., 275: 10484-91.

Nishikawa, A., E. Murata, M. Akita, K. Kaneko, O. Moriya, M. Tomita, H. Hayashi, 1998. Role of macrophages in pro-grammed cell death and remodeling of tail and body muscle *of Xenopus laevis* during metamorphosis. Histochemistry. Cell Biology, 109: 11-17.

Page, H.B., S.R. Voss, A.K. Samuels, J. Smtth, V. Putta, C.K. Beachy, 2008. Effect of thyroid hormone concentration on the transcriptional response underlying induced metamorphosis in the Mexican axolotl *(Ambystoma)*. BMC Genomics, 9: 78.

Phillips, M.E., J.E. Platt, 1994. The use of a marker of thyroxine induced apoptosis in cultured *Rana catesbeiana* tail tips. Gen. Comp. Endocrinol., 95: 409-415.

Purrello, M.N, M. Scalia, Corsaro, C., Di Pietro, C., Piro, S., Sichel, G., 2001. Melano-synthesis, differentiation, and apoptosis in Kupffer cells from *Rana esculenta.* Pigment Cell Res., 14: 126-131.

Saad, A.H., A. Abu-Taira, F. EI-Badry, 2005. Embryonic development of heteroploid *Bufo regularis* V (Amphibia, Bufonidae) III. Natural apoptosis during lymphocyte development. Egypt. J. Zool., 45: 55-76.

Sachs, L.M., S. Damjanovski, P.L.Jones, Q. Li, T. Amano, S. Ueda, Y.B. Shi, A. Ishizuya-Oka, 2000. Dual functions of thyroid hormone receptors during *Xenopus* development. Comp. Biochem. Physiol. B. Biochem. Mol. Biol., 126: 199-211.

Saelim, N., D. Holstein, E.S. Chocron, P. Camacho, J.D. Lechleiter, 2007. Inhibition of apoptotic potency by ligand stimulated thyroid hormone receptors located in mitochondria. Apoptosis, (10): 1781-94.

Sanders, E.J., M.A. Wride, 1995. Programmed cell death in development. Int. Rev. Cytol., 163: 105-173.

Sedra, S.N., M.PI. Michael, 1961. Normal table of the Egyptian toad *Bufo regularis* Reuss, with an addendum on the stand-ardization of the stages considered in previous publications. Ceskoslovenska Morfol., 9: 333-351.

Shi, Y-B, L. Fu, T. Hasebe, A. Ishizuya-Oka, 2007. Regulation of extracellular matrix remodeling and cell fate determination by matrix metalloproteinase stromelysin-3 during thyroid hormone-dependent post-embryonic development. Pharmacology and Theraputics., 116: 391-400.

Shook, D.R., C. Majer, R. Keller, 2004. Pattern and morphogenesis of presumptive superficial mesoderm in two closely related species, *Xenopus laevis* and *Xenopus tropicalis*. Dev. Biol., 270(1): 163-85.

Szalewicz, A., B. Strzelczyk, M. Sopel, A. Kubicz, 2003. The 35 kDa acid metallophosphatase of the frog *Rana esculenta* liver: studies on its cellular localization and protein phosphatase activity. Acta Biochim. Pol., 50(2): 555-66.

Taniguchi, Y., T. Sugiura, A. Tazaki, K. Watanabe, M. Mochii, 2008. Spinal cord is required for proper regeneration of the tail in *Xenopus* tadpoles. Dev. Growth Differ., (2): 109-20.

Taylor, A.C., J.J. Kollros, 1946. Stages in the normal development of *Rana pipiens* larvae. Anat. Res., 94: 7-23.

Tsuchiya, Y., S. Murai, S. Yamashita, 2005. Apoptosis-inhibiting activities of BIR family proteins in *Xenopus* egg extracts. FEBS J., (9): 2237-50.

Veldhoen, N., D. Crump, K. Werry, C.C. Helbing, 2002. Distinctive gene profiles occur at key points during natural metamorphosis in the Xenopus laevis tail. Dev. Dyn., 225: 457-468.

Vignal, E., P. De-Santa Baebara, L. Guemar, J.M. Donnay, P. Fort, S. Faure, 2007. Expreesion of RhoB in the developing *Xenopus laevis* embryo. Gene Expr. Patterns., 7(3): 282-8.

Webster, D.A., J. Gross, 1970. Studies on possible mechanisms of programmed cell death in the chick embryo. Devl. Biol., 22: 157-184.

Wyllie, A.H., 1980. Glucocorticoid-induced thymocyte apoptosis is associated with endogenous endonuclease activation. Nature., 284: 555-556.

Zorn, A.M., J. Mason, 2001. Gene expression in the embryonic *Xenopus* liver. Mechanism of Development., 103: 153-157.